Design & Testing of TRL5 IPEx Actuators

Casey J. Clark
LASSO 2, Kennedy Space Center
Kennedy Space Center, FL 32899
321-867-5666
casey.j.clark@nasa.gov

Jonathan Drew Smith
NASA, Kennedy Space Center
Mail Stop: UB-E
Kennedy Space Center, FL 32899
321-867-8726
jonathan.d.smith@nasa.gov

Andrew J. Nick
NASA, Kennedy Space Center
Mail Stop: UB-E
Kennedy Space Center, FL 32899
321-867-4873
andrew.j.nick@nasa.gov

Victoria V. Ortega
NASA, Kennedy Space Center
Mail Stop: UB-E
Kennedy Space Center, FL 32899
321-416-7228
victoria.v.ortega@nasa.gov

Jason M. Schuler
NASA, Kennedy Space Center
Mail Stop: UB-E
Kennedy Space Center, FL 32899
321-867-7854
jason.m.schuler@nasa.gov

Jeffrey E. Dyas
NASA, Kennedy Space Center
Mail Stop: NET-E0
Kennedy Space Center, FL 32899
321-867-8609
jeffrey.e.dyas@nasa.gov

John Lahl
LASSO 2, Kennedy Space Center
Kennedy Space Center, FL 32899
321-867-XXXX
john.lahl@nasa.gov

Abstract— **NASA is advancing In-Situ Resource Utilization (ISRU) by focusing on missions aimed at establishing sustainable infrastructure on the Moon and Mars. On the Moon, regolith serves as the most abundant resource. To support ISRU objectives, a 30-kg-class robot called ISRU Pilot Excavator (IPEx) is being developed to excavate 10,000 kg of lunar regolith during a future technology demonstration mission. IPEx uses novel excavation tools, called bucket drums, which are hollow cylinders with scoops staggered around the outside. Regolith is collected with the scoops and flows into the drum where it is captured by an internal baffle system. The excavator can then transport the regolith in the drum and reverse the direction of the drum rotation to dispense the regolith out. IPEx uses two sets of bucket drums that dig simultaneously in opposing directions and results in counteracting excavation forces. This combination of bucket drum excavation tools and counteracting excavation forces enables low mass robotic excavators to effectively dig in reduced gravity environments. This is a significant departure from terrestrial excavators that rely on high mass to produce tractive forces to counteract the forces of excavation.**

IPEx is made up of several custom actuators that all need to be verified for their intended application. This paper focuses on the initial design, testing and modifications of three actuators: the mobility actuator, the shoulder actuator, and the excavation actuator.

Each actuator was tested under four separate test profiles: ambient motor characterization, hot and cold motor characterization, accelerated life test (ALT), and concept of operations (ConOps) test. The motor characterization tests enabled derivation of torque equations for each actuator to estimate output torque without implementing sensors. The accelerated life tests were successful for each actuator and verified the motors' ability to survive the mission. For the ConOps test, only the bucket drum actuator performed a complete ConOps without the need to restart the test. Overall, the first series of testing resulted in various failure modes and minor design alterations for each actuator. The test results, failure modes, and design alterations are highlighted within this paper. This paper focuses on discussing the mobility, excavation, and shoulder actuator design, testing principles, and results that qualified it as a TRL 5 system.

979-8-3503-5597-0/25/$31.00 ©2025 IEEE

TABLE OF CONTENTS

1. INTRODUCTION

NASA's goal of sustainable exploration of the Moon and Mars will be enabled by locally sourced resources. This approach will reduce the supplies launched from Earth and is known as In-Situ Resource Utilization (ISRU). Many of the resources available on the Moon can be found in the outer layer of loose rocky material known as regolith. The regolith can be excavated and processed to extract desired resources, such as oxygen. To date, NASA missions have only excavated tens of kilograms of lunar regolith and excavation has never been performed by a dedicated excavation technology, rather only as a secondary function of an exploration rover or sampled by an astronaut.

Swamp Works at Kennedy Space Center (KSC) specializes in the development of ISRU robotics and regolith simulant testing. NASA annually funds various projects under the Space Technology Mission Directorate (STMD) Game Changing Development (GCD). STMD GCD announces gaps in technology that need to be closed or investigated to reduce risk in future missions. In 2021, the Swamp Works team received funding for a proposal to develop an excavation robot called the ISRU Pilot Excavator (IPEx), which aims to

tackle several challenges in the areas of Advanced Materials, Structures, & Construction (AMSC) and In-Situ Resource Utilization (ISRU) technologies.

The alpha configuration of IPEx can be oberved in Figure 1.

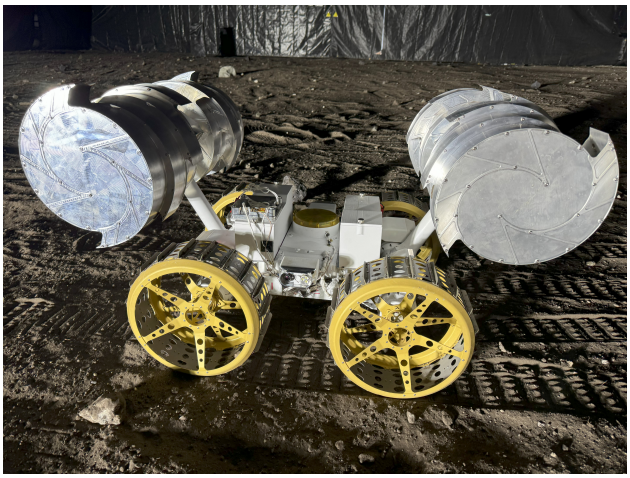

Figure 1. Alpha configuration of IPEx

The IPEx will be NASA's first lunar surface robot specifically designed with the reliability and efficiency to demonstrate the excavation of large quantities of regolith. This capability is critical to sustained lunar mission success. By the end of the decade, the excavation needs will increase from sampling levels to tens or hundreds of tons of regolith per year. Full-scale sustained ISRU and construction of infrastructure will increase that amount to thousands of tons of regolith per year. To achieve IPEx to excavate 10,000 kg of lunar regolith on a Commercial Lunar Payload Services (CLPS) demonstration mission. IPEx is proposed to be made available as Government Furnished Equipment (GFE) to LIFT-1 or other future lunar missions.

The ISRU Pilot Excavator (IPEx) proposal awarded has two major goals:

1. 1. Design and build a flight ready robotic system to demonstrate excavation, transportation, and delivery of 10 metric tons of loose granular lunar regolith as required for an in-situ pilot processing plant.

2. 1.2. Support the integration, flight operations, and reporting of the lunar surface demonstration.

IPEx incorporates key design features from the Regolith Advanced Surface Systems Operations Robot (RASSOR) 2 excavator, as shown in Figure 2 [1].

IPEx, as well as RASSOR, utilize innovative excavation tools known as bucket drums that are hollow cylinders with scoops arranged around the exterior to collect regolith. The excavator lowers arms attached to the bucket drums and rotates them once they make contact with the surface. The material is then collected by the scoops and flows into the drum, where it is captured by an internal baffle system. The excavator can then raise its arms back up and transport the regolith. Reversing the direction of the drum rotation dispenses the regolith out. IPEx uses two sets of bucket drums, one on each side of its chassis, to dig simultaneously in opposing directions and results in counteracting excavation

Figure 2. RASSOR 2 with it's Arms Raised in the Big Bin at Swamp Works, NASA KSC

forces [2]. This combination of bucket drum excavation tools and counteracting excavation forces enable low mass robotic excavators to effectively dig in reduced gravity environments [3]. This is a significant departure from terrestrial excavators that rely on high mass to produce tractive forces to counteract the forces of excavation.

The mission will be conducted semi-autonomously and occur over an 11-day span. IPEx will excavate autonomously using Autodig algorithms that estimate the amount of regolith collected based upon the excavation motor's current [4]. This project will design, build and test 2 versions of IPEx. The first is a Technology Readiness Level (TRL) 5 system that will be broken into different sub-systems and tested in relevant environments to increase the TRL to 6, which will become the flight version.

The mobility, excavation, and shoulder actuator are the three main subsystems that are discussed in this paper. The mobility actuator drives the wheels, the excavation actuator drives the bucket drums, and the shoulder actuator drives the arms holding the bucket drums. Each actuator has their respective test matrices and requirements driven by the ConOps.

2. Concept of Operations

The IPEx mission's goal is to prove the advancement in state-of-the-art (SOTA) for off-Earth excavation technology by excavating up to 10,000 kg of regolith, at a rate of 42 kg/hr, and covering a total distance of 70 km while operating in the South Pole region of the Moon over 11 days [5]. IPEx is not required to survive the lunar night.

The ConOps for the IPEx mission is cyclical in nature. After landing on the moon IPEx will deploy from the lander and perform a teleoperated slow driving mapping routine. The area of interest is a half-circle around the lander with a radius of approximately 15 m where a dig site and dump site will be identified. Between the dig and dump site a driving path will be selected that avoids identified rock and crater hazards. IPEx will drive an arcing path that maintains constant view of the lander from the side camera for absolute localization using fiducial targets. The arcing path will allow IPEx to simulate a 100 m drive between the dig and dump sites, which is a minimum requirement from oxygen production teams.

After the mapping is completed, IPEx will drive back and forth from the dig and dump site following the 100m arcing path until the battery is depleted. Once the battery is depleted, IPEx will dock to the lander and recharge using a wireless charger. This flow will be repeated until IPEx excavates 10 metric tons of lunar regolith over a span of 11 earth days.

Due to the nature of an excavator, IPEx will need to be dust tolerant. The main areas of concern for dust collection include the thermal system, charging system, and the actuators. The thermal system consists of a phase change material connected to a radiator plate and mitigates dust through implementation of an actuated cover that protects the radiator surface from dust. For the charging system, a wireless charger was implemented to recharge the excavator at the lander, eliminating the need for a dust tolerant connector. For the actuators, felt seals and a labyrinth seal path were implemented, as discussed later in this paper.

The ConOps for IPEx was recreated with RASSOR 2 to record the current draw on the battery and actuators to estimate the loads imparted on the system. A 1-dimensional scaling factor of approximately 0.7 was then used to estimate the physical size of IPEx based on testing with RASSOR 2. The loads estimated and 0.7 scale factor was used to determine mass, speed, and physical size of IPEx to then estimate power draw [5]. This data was incorporated into the design of the actuators as later discussed.

3. Actuator Design Philosophy

The IPEx team used the Helical Design process defined at the KSC Swamp Works lab [6]. This process utilizes a design, test, and iterate approach. The first actuator iteration was based on the RASSOR 2 design with a linear scale factor of 0.7 and is referred to as the Gen 1 actuator (depicted in Figure 3). The Gen 1 actuator test results later informed the current design of the IPEx actuators.

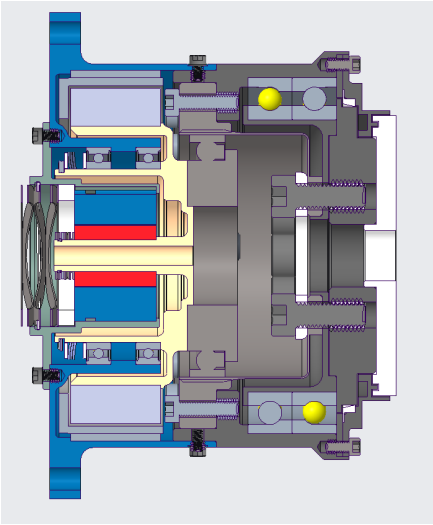

Figure 3. Gen 1 Actuator - Cross-section

The team designed the Gen 1 actuator to meet the torque and speed requirements of the shoulder actuator, while maintaining a form factor suitable for testing individual components in a cryo-vac chamber. This was important in the design of the Gen 1 actuator to understand the inefficiencies associated with the motor, motor bearings, harmonic drive, output bearings, dust seals, and resolver. While manufacturers provide performance data, such as motor curves and gear efficiency, these values are typically based on specific grease, temperature, and Earth-based pressures; performance data in a lunar environment was needed to inform decisions for future iterations. Both JSC and JPL Subject Matter Experts (SMEs) were consulted on motor feedback options and grease selection.

The Gen 1 actuator was a direct drive motor to harmonic drive with resolver feedback system. A resolver was selected based off the VIPER actuator design for commutation, position, and speed control feedback. The JPL team suggested a grease plating lubrication process to apply a thin coat of Braycote vacuum rated grease to the bearings and gearing components.

The Gen 1 actuator was tested in the Small Space Environment Dynamometer (S-SED) [7]. Testing was conducted as individual components and as a full system. Some of the unknowns explored included how the grease plating affected performance in the bearings and gears at different temperatures, how the resolver performed at lower speeds, and the drag associated with the dust seals

The drag due to grease plating as negligible between -70 C and 20 C. Due to the direct drive nature of the design, a max gear ratio with the harmonic drive gearset was selected for max torque output and to increase the motor speed during low velocity operations . The small gear ratio relative to other designs that include a planetary gearbox in combination with a harmonic drive requires that the motor operate as low as 50 RPM in some cases. A typical Hall effect sensor for speed control was assumed to be insufficient due to the low motor speeds and therefore the resolver was implemented. The resolver itself had many issues including noise and drift. Using a SED motor controller, Elmo Motion Controller, the team was able to get the Gen 1 actuator operational.

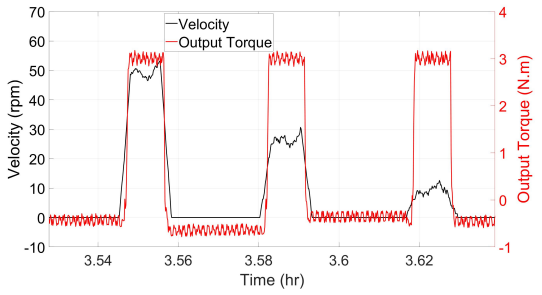

Figure 4. Low Speed Control with Hall Effect Sensors

During testing the noise of the resolver was not ideal and it was decided to attempt a Hall only motor for commutation, velocity, and position feedback. After running several low velocity tests with an acceptable resultant control profile, it was decided to remove the resolver from the baselined design and move forward with Hall effect sensors only. The low speed data of this test can be observed in Figure 4.

Sealing to keep regolith dust from entering the actuators was the last concern. The current space industry practice is a layered three stage approach utilizing a labyrinth as the outer most system followed by a felt seal and finally a PTFE lip

seal. Dust prevention was not tested during this Gen 1 test campaign but drag torque from the seals was of interest for the future design. Several tests were conducted at various temperatures, torques, and speeds with and without seals. The maximum drag recorded was 0.03 Nm. The drag varied throughout the range of tests but since it was less than 1% of the overall load, it was not a concern.

This Gen 1 design and test campaign provided answers to many of the unknowns and provided data for the design of the three main actuators for the IPEx excavator.

4. Actuator Design

IPEx is designed to dig and dump lunar regolith, navigate over rocks, withstand falls, and operate with limited obstacle detection. The mobility actuators drive the wheels, the excavation actuator drives the bucket drums, and the shoulder actuator drives the arms of the excavator. The actuators designed prioritize dust tolerance and robustness while maintaining simplicity. Furthermore, the actuators tested on Earth use the same design intended for the lunar mission, resulting in more than six times the performance margin in most cases due to Earth's gravity, though this comes at the expense of increased mass. The placement of the actuators can be seen in Figure 5.

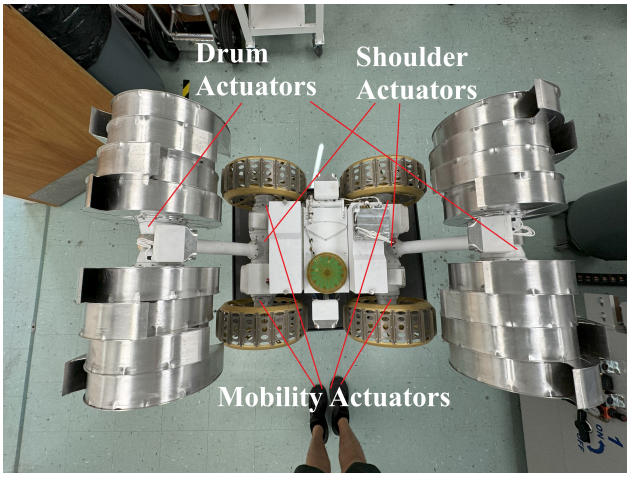

Figure 5. Actuator Labels on IPEx Alpha Configuration

Mobility Actuator

The mobility actuators are required to have high reliability since they are responsible for driving the excavator to and from the dig and dump site and back to the lander. During the entire 11-day mission IPEx will drive approximately 70 km, mostly over the same terrain due to the cyclic nature of the con-ops. To accomplish this a nominal drive speed of 30 cm/s is required as well as traversing rocks up to 7.5 cm in height and inclinations up to 15 degrees.

The cross-section of the mobility actuator is shown in Figure 6.

The design of the mobility actuator is very similar to the Gen 1 actuator. Given that the overall mass of IPEx is required to be in the 30 kg class range, the mobility actuator mass allocation was approximately 0.85 kg per actuator. This mass allocation drove the team to a very compact solution. A brushless DC ThinGap LSI 75-12 motor with Honeywell

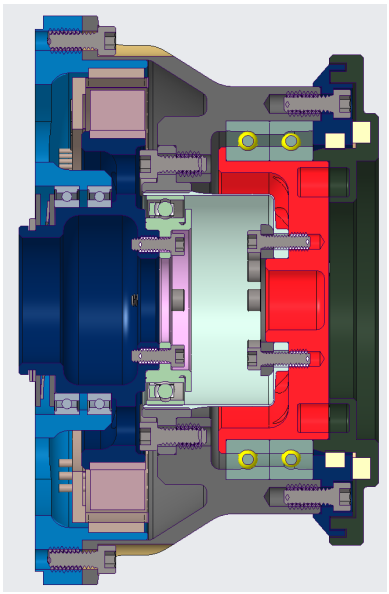

Figure 6. Mobility Actuator - Cross-Section

SS511AT Hall effect sensors, a Harmonic Drive CSF 14-80LW gearset, SKF 71809 angular contact back-to-back bearings on the output to react to loads imparted into the actuator from the environment, EZO 6706 deep groove bearings for the motor rotor, and a Nomex dust seal were incorporated. Output bearings were sized to fit over the harmonic drive flex cup and input bearings were stacked close together and preloaded with a wave spring. The wave springs were sized such that the axial force generated by the harmonic drive wave generator would not overcome the spring force and therefore keep the motor rotor and wave generator axially positioned. Commonality of fasteners was also desired across the IPEx; 4- 40 A286 screws with locking Nitronic 60 helicals were used throughout the design. Several exceptions were, including the use of 2-56 fasteners for the harmonic drive flex cup and wave generator.

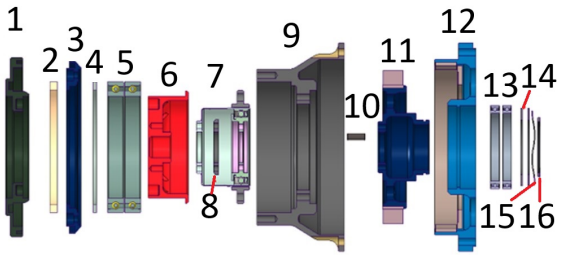

Figure 7. Mobility Actuator - Cross-Section

An exploded view of the components of the mobility actuator can be seen in Figure 7. The component labels are:

1. Output Flange
2. Nomex dust seal
3. Output bearing clamp
4. Output bearing shim
5. Output bearings
6. Output
7. Harmonic Drive
8. Flex Spline Clamp
9. Actuator housing
10. Shear pin
11. Motor rotor
12. Motor housing
13. Motor bearings
14. Motor shims
15. Wave spring
16. Snap ring

Excavation Actuator

The bucket drum excavation force test campaign 8 performed on RASSOR 2 showed that forces due to excavating regolith did not vary significantly due to the gravity difference. A trade study was performed to determine if two smaller actuators should drive the bucket drums on each side of the arm or a single actuator. The benefits for two smaller actuators included the ability to independently drive the drums and heritage from the RASSOR 2 design. The downsides of two independent actuators were mass, increase in part count, and additional motor controllers and wires. From this trade study a single actuator was baselined.

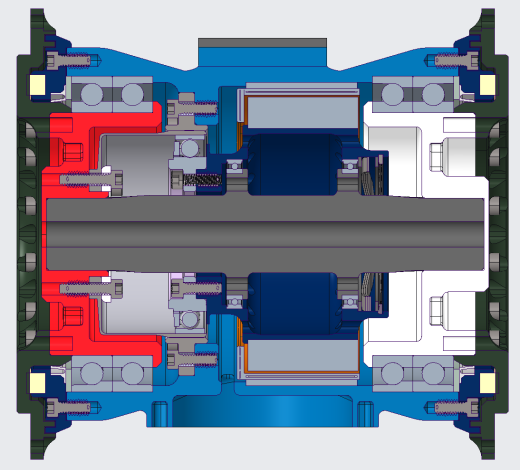

Figure 8. Excavation Actuator - Cross-Section

Although a single actuator had benefits, it presented its own challenges. The biggest challenge to overcome was torque transfer from one side of the actuator to the other. The solution was to run a shaft from the output of the harmonic drive through the middle of the actuator to the other side. Using the harmonic drive wave generator without the Oldham coupler allowed for a sizable shaft to run the length of the actuator. However, this shaft precluded the ability to ground the motor rotor independent of the actuator output. The team ended up using this torque transfer shaft as the ground of the motor rotor by adding features to mount bearings. The cross-section (shown in Figure 8) illustrates how the output of the harmonic drive flex cup transfers torque to the shaft running the length of the actuator that attaches to a flange on the opposite side. The motor rotor bearings are mounted to this same shaft and act as the ground.

The torque transfer shaft mates with the output flanges by a Polygon Profile P3 18 g6/1.4 connection. This connection was chosen for its ability to be machined into a blind hole and allowed for easily assembling mating parts.

Analysis and testing in the SED chamber and Earth excavation demonstrations were conducted to ensure this design performed as expected.

Shoulder Actuator

The shoulder actuator is a derivation of the excavation actuator utilizing many of the same components. This design made an exception on the power needed for full earth-based testing. To maintain the size of the motor, the team decided to load the arm to 30% of the full load during earth testing. Both the excavation and shoulder actuator include a Harmonic Drive CSF 20- 160LW gear set, a ThinGap LSI 75-30 brushless DC motor with Hall effect sensors, deep groove ball bearings on the motor rotor, and SKF 71812 angular contact bearings on the output. The primary differences are that the arm actuator includes a power-off brake and lacks the internal torque-transmitting shaft. The brake keeps the arm from back-driving when power is not applied and will save energy while driving between dig and deposit operations. The shoulder actuator design challenge was to have wire pass through the passive side of the actuator as well as the driven side. Many of the wires run through the passive side of the actuator into a wire containment feature. This feature keeps the wires from interfering with the motor rotor. The power-off brake wires are the only wires that get passed through the active side of the shoulder actuator. The cross section of the shoulder actuator is depicted in Figure 9.

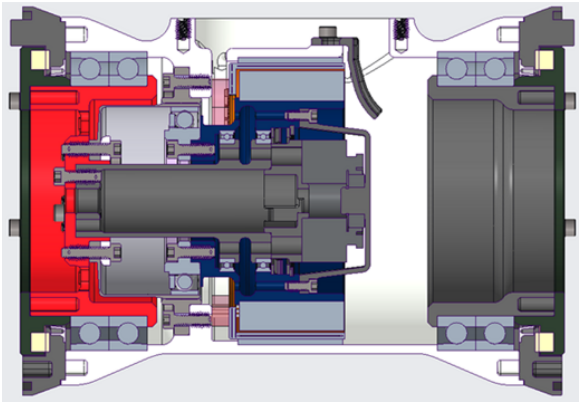

Figure 9. Shoulder Actuator - Cross-Section

5. TEST PLAN

The scope of this plan is focused on the Brassboard Version integration and testing to be performed on the IPEx actuators. This includes subsystem testing to support requirement development for the flight version of IPEx.

IPEx is a sub-Class D payload per NPR-8705.4 “Risk Classification for NASA Payloads”[8]. The flight payload will be designed and tested per ARC-STD-8070.1 “Space Flight System Design and Environmental Test .” The brass-board unit (encompassed in this plan) is not required to meet ARC-STD- 8070.1, but recommended test requirements will be provided as reference to support successful testing regiments [9].

The testing approach will focus on achieving 1) system performance, 2) model grounding, and 3) ground validation. To reach TRL 6 maturity , there must be a subsystem and/or system demonstration in a relevant environment. Both ’Demonstration’ and ’Relevant environment’ for this project will take into consideration cost and schedule and will be defined for each test with justification. The tests will be broken into subsystem level tests, with additional assembly level tests done on critical assemblies such as the actuators and wheels. Some subsystem tests, like the Mobility system and the Regolith Delivery System, will be done with the alpha configuration IPEx.

Actuator testing, which includes the wheel, shoulder, drum actuators and radiator cover, consists of four unique tests. Each actuator will be configured separately in performing these tests. The actuators will be exposed to vacuum for all tests and include regolith simulant for the ConOps test. These

tests will be outlined in the test procedures. TC1 through TC4 encompass the KSC Actuator Qualification Test campaign. The tables for each of the tests are tabulated in the appendices section of this paper due to their size.

The tables for each of the following tests are tabulated in the appendices section of this paper due to their size.

TC1 - Actuator Characterization Testing: Define torque curves at no load and at incrementally increasing load cases up to expected max load at nominal temperature (median of the ConOps temperatures provided by JPL thermal analysis team for each actuator) and varying speeds and voltages. These will be placed in a database to support optimization of the next version of each respective actuator. This test will serve to verify nominal operations of a newly assembled actuator for final integration.

TC2 - TVAC Operational Testing: Test the actuators at high and low end operational temperature ranges (provided by JPL thermal analysis team for each actuator and include a +/- 10 degrees of margin). Two cycles with four-hour dwell periods after temperature stabilization with a transition rate prescribed by the JPL thermal analysis team was followed (¡ 4 C/min). During dwell periods, collect motor characterization data at temperature extremes. After completion of TVAC testing, re-perform a tailored motor characterization test at nominal temperature to see deltas. This test was done in serial as TC1 with the same test configuration. After finishing this test, the actuators were taken out of the chamber and disassembled to look for visual deltas to the assembly prior to testing.

TC3 - Accelerated Life testing: Test the actuators to failure

1) Perform usage rate accelerated life testing for the bucket drum and shoulder actuator, which entails running each actuator continuously at 2-sigma loads (68% of max expected mission load) at the max expected mission temperature and providing the minimum input voltage of the expected usage at 2x ConOps total revolutions (rerun baseline test after every 2x ConOps revolutions).

2) Concurrently with 1, perform accelerated life testing for the wheel actuators by providing minimum input voltage, running at max expected mission temperature at 3-sigma loads (99.7% of max expected mission load) for the whole mission duration of the expected usage at 2x ConOps total revolutions (rerun baseline test after every 2x ConOps revolutions)..

These tests were performed with the same build as TC1 and TC2 tests.

TC4 - ConOps Testing: Incorporate a dust cup with a newly assembled actuator, perform ConOps testing with nominal load cases for each actuator, varying the temperature based on the rate as prescribed by JPL thermal analysis team (as hot as the chamber can allow). The testing would nominally proceed as follows:

1) Perform a functional test to compare to TC1

2) Run 332 dig and dump cycles, transitioning temperature at the expected mission rate. Starting temperature is the starting mission temperature for each actuator respectively.

3) Perform a functional test to compare to TC1.

4) Rerun steps 1 through 3.

5) Take out of chamber and disassemble to inspect seals and dust accumulation.

Four separate builds of each of the four types of actuators are required to be tested, for a total of sixteen actuators that need to be built to perform the tests. Two actuators of each type will be tested under TC1, TC2 and TC3 test criteria, while the other two actuators will be reserved for TC4 test criteria.

6. Facility & Apparatus

The S-SED, depicted in Figure 10 at Swamp Works was originally designed for testing of Bulk Metallic Glass Gears (BMGG). Over the years, it has been used to test various other projects, including a dust test involving a motor for Volatiles Investigating Polar Exploration Rover (VIPER). IPEx's mobility actuator and radiator hinge motor are both tested in this chamber.

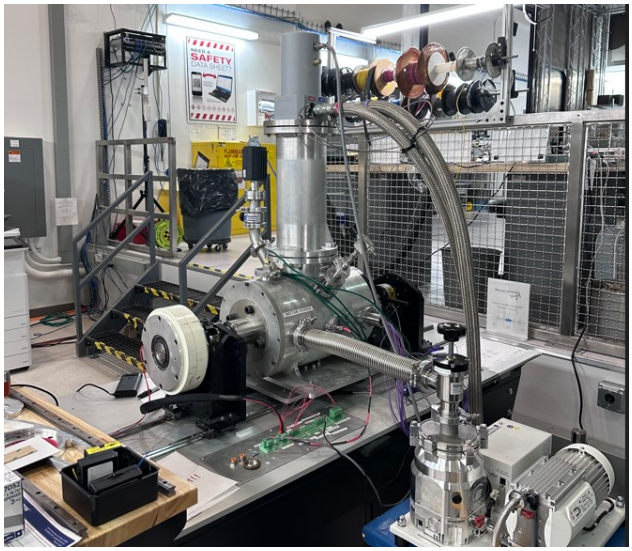

Figure 10. Small Space Environment Dynamometer (S-SED) located at Swamp Works, KSC, FL

The S-SED utilizes a variety of sensors and other hardware to perform cold tests of actuators. The chamber pumps to approximately 50 milliTorr using a roughing pump, at which point a turbo pump is activated to get the chamber to 0.5 milliTorr. A cryo-cooler is used to conductively cool a test article through its cryohead.

Thermocouples, RTDs, and diodes are used to monitor the temperature of the cryohead, cold plate, and various places on the actuator. Heaters, either cartridge or adhesive, are carefully placed symmetrically along the actuator to minimize the temperature gradient. The heaters are controlled through a relay that shuts off if the cryohead reaches a temperature above 30C. A static torque sensor is used in conjunction with an electromagnetic particle brake to perform closed loop control of torque on the actuator.

A cross section of the test configuration of the mobility actuator installed in the S-SED can be seen in Figure 11. The main components of the test set up are as follows:

1. Mobility Actuator
2. Coldplate
3. Cryohead (cold-finger)
4. Cryohead extension
5. Ferrofluid rotary feedthrough
6. Output torque sensor
7. Magnetic particle brake

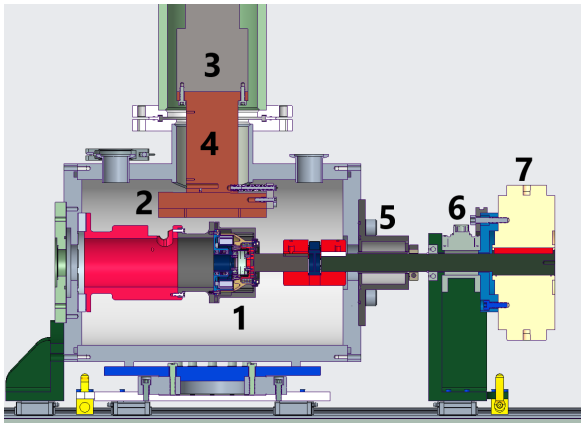

Figure 11. Cross section of the CAD of the Mobility Actuator installed in the S-SED

The motor is controlled with a motor controller and tuned in proprietary software prior to testing. The S-SED is currently capable of interfacing with Elmo and ESI motor controllers via EtherCAT, and CAN through a FPGA, respectively. The SED is capable of interfacing with hall effect sensors and incremental and absolute encoders.

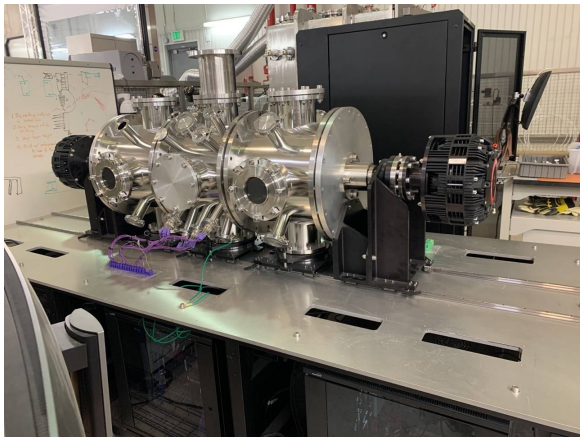

Figure 12. Large Space Environment Dynamometer (L-SED) located at Swamp Works, KSC, FL

In 2020, a larger chamber (depicted in Figure 12), was designed to test a mobility actuator for the Lunar Terrain Vehicle (LTV). This chamber is composed of three individual sections, approximately 160L in volume each. The LTV actuator tested was dual output, therefore the large space environment dynamometer (L-SED) was designed with brakes on both sides. The original brakes for the L-SED chamber were pneumatic, however it is capable of swapping out torque sensors and electromagnetic particle brakes depending on the loads required by the actuator being tested.

7. PROCEDURE

The actuator's outer surface is first cleaned thoroughly with acetone and isopropyl alcohol. Once clean, adhesive thermocouples are symmetrically placed. Depending on the actuator being tested, adhesive or cartridge heaters are used. If adhesive heaters are used, then they will be installed prior to thermal strapping. Cartridge heaters are installed during the thermal strapping process as they need to be secured with band clamps.

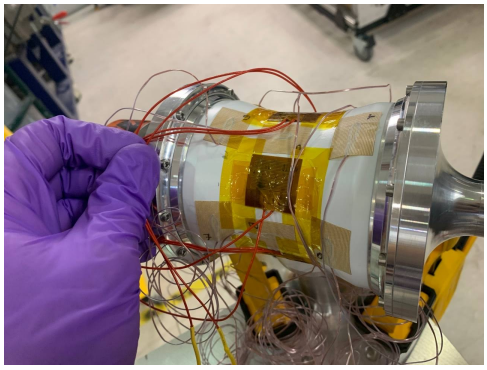

Figure 13. Bucket Drum Actuator Strapped with Thermocouples and Adhesive Heaters

A bucket drum actuator, fully interfaced with thirteen thermocouples and four adhesive heaters can be seen in Figure 13. Once thermocouples have been installed, the actuator is wrapped in copper straps and secured with band clamps. The number of straps varies greatly between tests and is dependent on the desired test temperature. The lower the test temperature, the more straps are required. Symmetry is vital when strapping, as the overall temperature gradient along the actuator needs to be minimal.

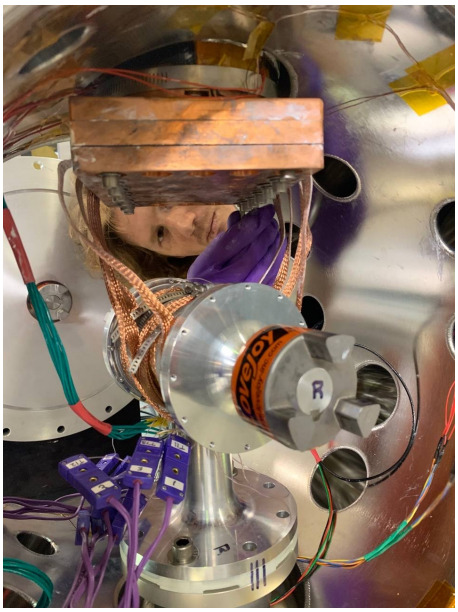

Figure 14. Bucket Drum Actuator Strapped with Copper Straps, Band Clamps and Installed in the L-SED

The actuator can be seen in Figure 14, installed onto it's pedestal, and strapped with thermal straps and band clamps.

8. RESULTS

Numerous tests at various voltages and temperatures were conducted for each test plan and actuator. Due to the extensive number of tests performed, only the results of the most relevant tests are presented in this section. The results are not organized chronologically by test execution but rather by the order in which the data was processed. Data processing influenced decisions that modified the test matrices for subsequent tests, and these decisions are noted in this section. The results for each test type are presented individually for all three actuators before moving on to the next test type. Equations developed from these test campaigns can be used during missions to assess actuator life decay and provide insight into regolith properties. Specifically for IPEx, these equations will assist in estimating mass and determining dig depth for autonomous excavation routines.

TC1 & TC2

TC1 & TC2 actuator characterization testing was originally performed at various voltages. The purpose of these tests was to empirically derive an equation for each actuator. The dependent variable would be the output torque (τ), as the current design for the IPEx rover does not include instrumentation that would directly allow for torque determination. Considering the output torque will be unknown on mission, the independent variables that could drive the output torque on any given actuator are its corresponding motor speed (ω), active current of the motor (I), bus voltage of the motor (V) and motor temperature (T). These equations were derived successfully for the mobility, excavation, and shoulder actuators.

Mobility Actuator—TC1 & TC2 for the mobility actuator have identical tables. The only difference is the corresponding temperature setpoint. The first series of TC1 & TC2 motor characterization tests performed on the mobility actuator were nominally set at ambient Earth temperature (20C for TC1) and the inferred temperature extremes calculated and provided by JPL (-35C and 40C for TC2). The TC1 & TC2 tests for the mobility actuator were performed in the S-SED.

The test profile for TC1 & TC2 for the mobility actuator is shown in Table 1 (see appendix). Each of these tests had the following constraints: 0 load represents the minimum load of the test stand, a maximum temperature deviation of $\pm$10C, log data every 250 ms, motor acceleration of 100 rpm/s, and the test waits until the actuator cools to test temperature before iterating the velocity.

A total of five TC1 & TC2 tests were performed on the mobility actuator. These tests consisted of two different voltages and three different temperature setpoints. Three tests at the same voltage and three individual temperature setpoints are compared to determine the effect voltage has on the current for a given torque/velocity profile. Two tests at two different voltages and the same temperature setpoint are compared to determine the effect temperature has on the current for a given torque/velocity profile. One data set is highlighted to show how an empirical equation is derived that will be used to predict the output torque on the actuator will be calculated on mission given the motor's parameters at any given moment.

Several tests were performed at the expected minimum (40.8V) and maximum (50.4V) bus voltages of the IPEx rover. Figure 15 shows the percent difference at each torque velocity setpoint.

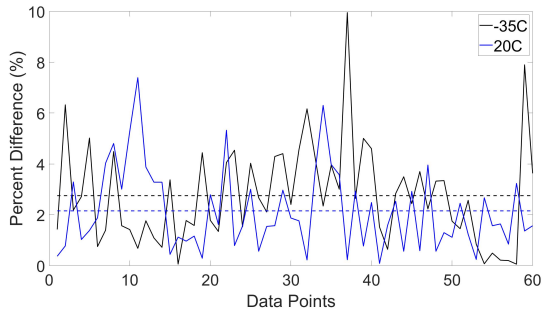

Figure 15. Mobility Actuator: Average percent difference

The dotted lines in Figure 15 represent the corresponding average percent difference between active current of the motor at two voltages for two temperature setpoints. The average percent difference is less than 3%, thus it was determined that voltage has little to no effect on the active current of the motor for a given speed, torque, and temperature profile. This led to the decision to conduct future tests at one voltage (40.8V) and eliminate voltage as an independent variable in the empirically derived equation for output torque on the actuator.

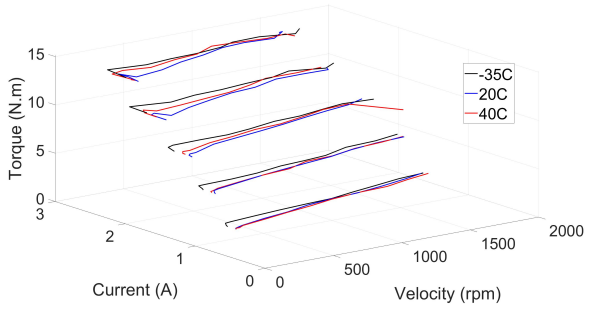

Figure 16. Mobility Actuator: TC1 & TC2 - Output Torque vs Current vs Velocity Experimental Data

Figure 16 shows the processed data for three tests conducted at 40.8V and three different temperatures: -35C, 20C and 40C. The controllability of the motor speed is drastically diminished at the low velocity setpoints (10 rpm, 25 rpm and 50 rpm). In addition, the controllability at lower speeds is further reduced for higher torques. This can be seen by the general trend of Figure 13.

The deviation between the data collected at 20C and 40C is overall sporadic and there does not appear to be a solid trend. Though, there does appear to be a trend when comparing the -35C data to both the 20C and 40C data; the current appears to be higher for the test conducted at -35C. This difference in current between tests at the same voltage shows that temperature does have a noticeable effect on the active current of the actuator for a given torque/velocity profile.

Unfortunately, no N-D polynomial, exponential nor logarithmic trend was found from the active current data between test temperatures. A single empirically derived equation for each actuator to calculate output torque with independent variables of motor velocity, active current of the motor and motor temperature is not feasible. Instead, a set of empirical

equations was derived to calculate output torque for each actuator. The number of equations for each motor will depend on the number of temperature setpoints for the TC1 & TC2 characterizations.

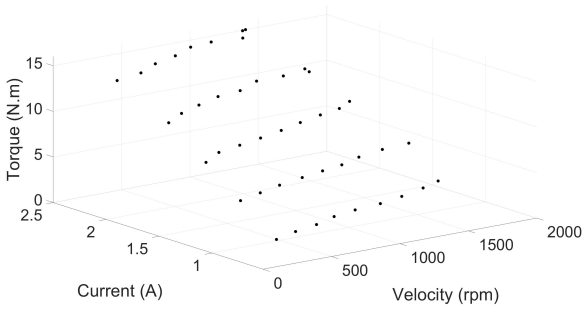

Figure 17. Mobility Actuator: Parsed experimental data for 20C and 40.8V

Figure 17 shows a parsed version of the data collected at 40.8V and 20C for the mobility actuator TC1 characterization; it excludes the lower velocities, as the trend in general is better when neglecting these velocities. The current at no load is also excluded from this data due to the unknown load/drag torque that is applied to the actuator. The current at no load is used only as health and life monitoring.

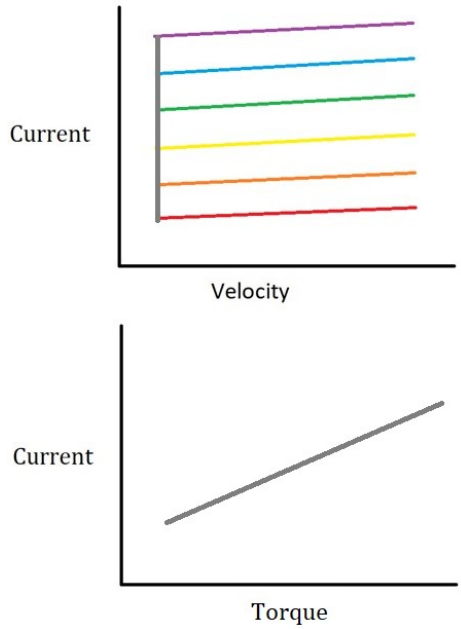

Figure 18. General Trend of Actuator Characterization between Velocity, Active Current and Output Torque

A general trend of the motor current behavior due to the applied velocity and torque is shown in Figure 18. The colors represent a constant applied torque. For a constant applied torque, the current linearly increases as the velocity increases. While for the same velocity, the current dramatically increases as the applied torque is increased. Two specific trends can be observed in the data: the slope of each regression line (individual colored lines) is relatively constant and the y-intercept of each regression line increases linearly with an increase in applied torque (gray line).

The active current of the motor I is dependent on the motor velocity ω, applied torque τ and motor temperature T

$$I = f(\omega, \tau, T). \tag{1}$$

As previously mentioned, an individual equation will be derived for each temperature, therefore Equation (1) is reduced to

$$I = f(\omega, \tau). \tag{2}$$

An equation for the motor current can be empirically defined using a 1-D polyfit:

$$I = m_\omega \omega + b_\omega. \tag{3}$$

Referring to Equation (3), m_ω is the average slope of the regression lines that estimate $I = f(\omega)$, while b_ω is the y-intercept of that regression line:

$$m_\omega = \sum_{i=1}^{n} \frac{m_{\omega_i}}{n} \tag{4}$$

$$b_\omega = f(\tau). \tag{5}$$

Within Equation (4), n refers to the number of torque setpoints (number of regression lines within Figure 18), and m_{ω_i} is the slope of each of the colored lines within Figure 18. When plotting the y-intercept b_ω with respect to applied torque τ, another linear trend appears. This allows for a second 1-D polyfit to be applied, resulting in:

$$b_\omega = m_\tau \tau + b_\tau, \tag{6}$$

where m_τ is the slope of this line and b_τ is the y-intercept of this line. Substituting Equation (6) into Equation (3) results in:

$$I = m_\omega \omega + m_\tau \tau + b_\tau \tag{7}$$

Finally, the empirically derived equation can be rearranged and solved for the applied torque in N.m for a motor velocity (ω) in rpm and current (I) in A:

$$\tau = \frac{I - m_\omega \omega - b_\tau}{m_\tau}. \tag{8}$$

An equation of this form is derived for each actuator at each temperature setpoint. An important note is this equation is valid within the torque/velocity test ranges. An example is provided using the data from the TC1 characterization of the mobility actuator at 40.8V and 20C.

$$\begin{aligned} m_\omega &= 3.384E-4 \ \frac{A}{rpm} \\ b_\tau &= 0.1049 \ A \\ m_\tau &= 0.1236 \ \frac{A}{N.m} \end{aligned} \tag{9}$$

This specific equation can be used for the mobility actuator at 20C for current values of 0.5A to 2.5A and velocities of 100rpm to 1700rpm. For this specific equation, any calculated torque value less than 3 N.m and more than 15 N.m is invalid. Using these values for m_ω, b_τ and m_τ with Equation (8), theoretical data was generated for the same active currents and motor speeds measured during TC1 at 40.8V and 20C. This theoretical data is compared to the experimental data.

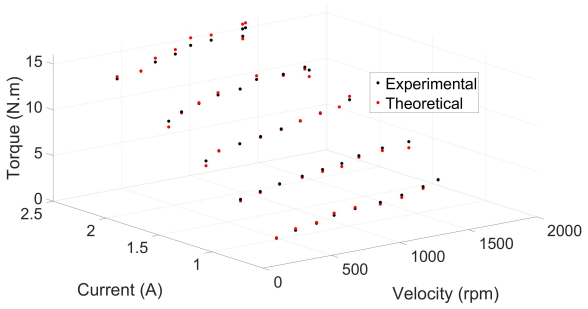

Figure 19. Mobility Actuator: TC1 40.8V and 20C - Experimental and Theoretical Data

Figure 19 shows the experimental and theoretical data overlaid on one plot for the TC1 motor characterization for the mobility actuator at 40.8V and 20C. The theoretical data was calculated using Equation (8) and the calculated example coefficients given in Equation (9).

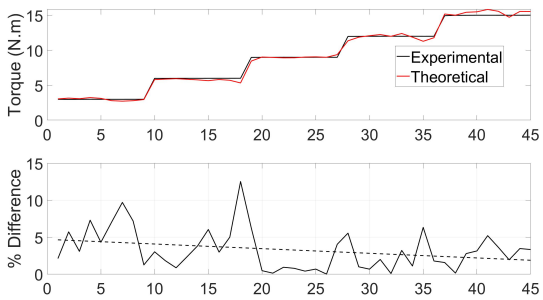

Figure 20. Mobility Actuator: Experimental vs Theoretical Comparison at 40.8V and 20C

Figure 20 directly compares the experimental vs theoretical data for the TC1 motor characterization for the mobility actuator at 40.8V and 20C. The x axis is simply the data points. There were 9 velocity setpoints (100:200:1700) used in the calculation of the data and 5 output torque setpoints (3:3:15). The dotted line in the bottom plot of Figure 20 is the linear regression of the percent difference. The equation is much more accurate for calculating higher output torques.

Excavation Actuator— The excavation actuator was tested within the L-SED, as it requires dual closed loop output torque control. The general constraints for the characterization tests are similar to those outlined for the mobility actuator, with the exception of waiting for the actuator to cool between torque/velocity setpoints and a 1-second log rate. These features were not implemented in the test program at the time the excavation actuator characterization tests were conducted. . The temperature of the excavation actuator did not rise more than 20C during each characterization for the subzero temperature setpoints and did not rise more than a fraction of a degree during characterization of ambient and hot temperature setpoints. Based on the 20C rise at the subzero temperature setpoint, the decision was made to update the code to include a wait between torque/velocity setpoints.

At the time these tests were conducted, there was concern with putting extra revolutions on the motor, therefore only 10s of data was recorded per velocity/torque setpoint. This only leads to only 10 data points at a 1s log rate, which is insufficient for creating a normal distribution (< 30). . Fortunately, the data was smooth post processing, though there may be a need for future characterizations of the excavation actuator. More more data points for future tests was needed, which dictated the decision to characterize the mobility actuator for 30s per velocity/torque setpoint.

There are two primary differences in the structure of the test plan in Table 2 compared to that of the mobility actuator (Table 1). Torque was iterated over a set velocity for the excavation actuator, while the opposite took place for the mobility actuator. The second difference in the test plans is we start with low velocities and low torques then increase them over time for the excavation actuator. The load reported in Table 2 refers to the total load on the actuator. Considering the excavation actuator is designed to drive both faces of the motor, the setpoint on each side is half of the value within the load column.

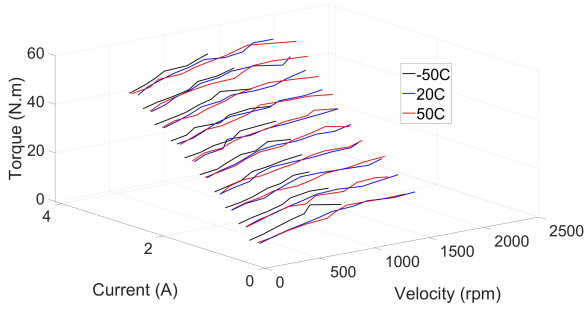

Figure 21. Excavation Actuator: TC1 & TC2 - Output Torque vs Current vs Velocity Experimental Data

Figure 21 displays the data collected at three different temperature setpoints. The same trends can be observed in this figure that were observed in the similar Figure 16 for the mobility actuator: the colder temperature results in higher current for the same velocity torque/setpoint and there is not a noticeable trend in behavior between the ambient and hot temperatures. The excavation actuator TC2 test at -50C unfortunately stalled during the 1600 rpm setpoint. This stall was later assumed to be associated with the axial loads generated from the wave generator. This led to an alteration of the excavation actuator design and is discussed in a later section.

To clarify, the derivation for Equation 8 is general and can be applied to any actuator for a given temperature. The excavation actuator TC2 data for 50C is used as an example to show how the theoretical values compare to the experimental data. The theoretical values are calculated from solving for the coefficients of Equation 8.

$$
\begin{aligned}
m_\omega &= 5.4903E-4\ \frac{A}{rpm} \\
b_\tau &= 0.2093\ A \\
m_\tau &= 0.0552\ \frac{A}{N.m}
\end{aligned} \tag{10}
$$

Using Equation 8 in conjunction with the coefficients listed in Equation 10, the theoretical data was generated and plotted with the experimental data.

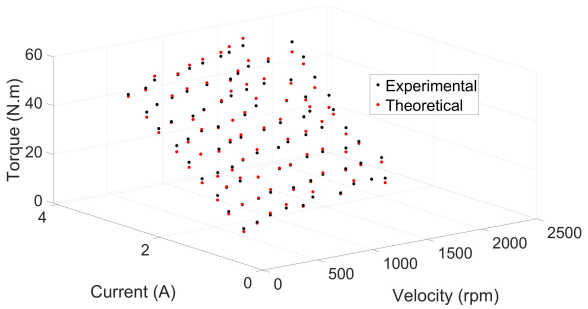

Figure 22. Excavation Actuator: TC1 40.8V and 20C - Experimental and Theoretical Data

Observing Figure 22, there is a promising relationship between the experimental and theoretical data, considering only 10 data points (1ms log rate for 10s) were used to compute the actual current, torque and velocity for each torque/velocity of the TC2 test.

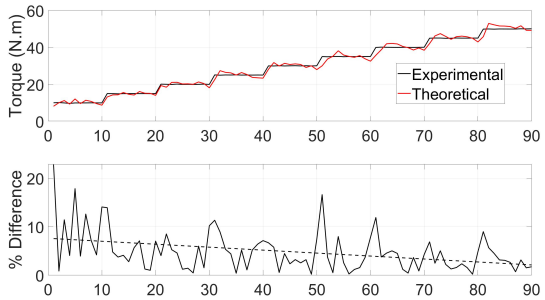

Figure 23. Excavation Actuator: Experimental vs Theoretical Comparison at 40.8V and 20C

The 5 N.m setpoint was excluded from the data as the torque sensors used to close the loop of the output torque control were reading less than 2% of their full scale value. Future tests will be conducted with more appropriately sized torque sensors. Referring to Figure 23, the percent difference between the theoretical and experimental values is exceptional considering the relatively oversized torque sensors used to conduct the test. Once again, there is a general trend of the percent difference decreasing for higher torque values.

Shoulder Actuator—The TC1&2 test plan for the shoulder actuator is identical to the excavation actuator test plan in Table 2. This is due to the analogous design between the two actuators. Due to time constraints on the test campaign, a condensed version of the test plan was implemented on the actuator, rather than performing a full TC1 & TC2 characterization of the shoulder actuator.

TC3

The TC3 accelerated life tests were overall successful for each of the three actuators. Though, some tests were iterative, while others were smooth (did not require restarts). Each of the three actuators demonstrated their ability to perform at least 1x of the mission ConOps total motor revolutions under 2-sigma to 3-sigma loads.

Mobility Actuator—The mobility actuator was tested using a 3-sigma accelerated profile. The 3-sigma load was based upon our nominal max load during operation, which corresponds to driving over a 1.32 cm rock. This rock size is a mean rock size taken from a Lunar rock distribution in the IPEx environment specification document. The goal of the accelerated life was to achieve a minimum 1x mission input revolutions, but ultimately continue to failure. The IPEx mission ConOps requires 5.7million inputs revolutions at the given parameters above. In total, the mobility actuator did successfully operate for over 1x mission input revolutions (6,547,036 input revolutions) over multiple inspections and disassembly.

Due to the axial movement of the motor rotor and the failure of the motor rotor bearing this test proves additional testing and design changes are required. This is discussed in a later section.

Excavation Actuator— The excavation actuator was tested using a 2-sigma accelerated profile. The 2-sigma load was based upon our peak load during the digging operation, which corresponds to digging and hitting rocks. The goal of the accelerated life was to achieve a minimum 1x mission input revolutions, but ultimately continue to failure. The IPEx mission con-ops requires approx. 880,000 inputs revolutions in a cyclic manner as predicted in the con-ops. In total, the bucket drum actuator did successfully operate for over 2x mission input revolutions (1.82 million input revolutions).

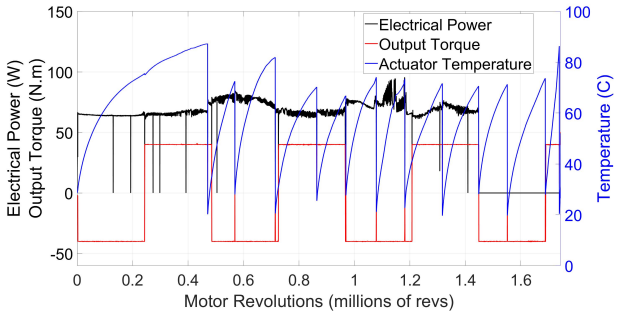

Figure 24. Excavation Actuator: TC3 Electrical Power, Output Torque and Actuator Temperature

As seen in Figure 24, the test was paused several times to allow the actuator to cool before resuming the test.

Shoulder Actuator—The shoulder actuator was tested using a 2-sigma accelerated profile. The 2-sigma load was based upon our nominal max load during operation, which corresponds to digging while actuating the arm. The goal of the accelerated life was to achieve a minimum 1x mission input revolutions, but ultimately continue to failure. The IPEx

mission con-ops requires approx. 337,000 inputs revolutions in a cyclic manner rotating from 0 to 90 degrees at the given parameters above.

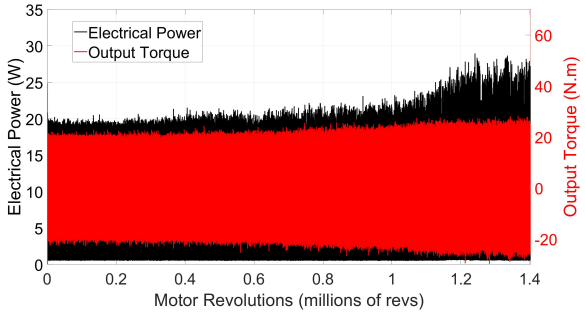

Figure 25. Shoulder Actuator: TC3 Electrical Power and Output Torque

In total, the arm actuator successfully operated for over 4x mission input revolutions (1,402,223 motor revolutions) without any issues.

The test was stopped at this point to move on to TC4 testing. Figure 25 begins to show wear of the actuator towards the end of the test which is well beyond the life needed for the mission ConOps. It was also noted an increase in the output load torque during the test which should have been a constant for the duration of the ALT.

TC4

ConOps testing was performed with a thermal profile defined by the JPL thermal team. The team provided a transient thermal model of the lunar mission for each actuator. A dust cup was included to simulate dust loading. Testing proved that a single felt seal provided enough protection from the regolith dust in a worse case scenario.

Mobility Actuator—The TC4 for the SN2 mobility actuator completed the entire test plan with several restarts. The first test stopped at 211,649 motor revolutions due to a current limit being reached. The second test stopped at 229,867 motor revolutions, again due to a current limit being reached. The third test went successfully and completed the remaining steps of Table 6, finishing with a combined total of 6,072,330 motor revolutions over all three tests.

JPL provided several transient thermal models of actuator temperatures based on the currently planned mission.

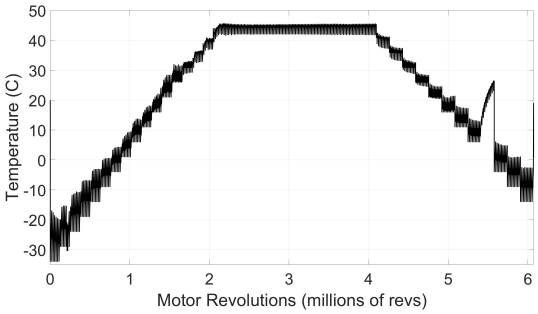

Figure 26. Mobility Actuator: TC4 Actuator Temperature

Figure 26 shows fully automated temperature control. The spike in temperature between 5 million and 6 million revs was the result of a typo in the test profile.

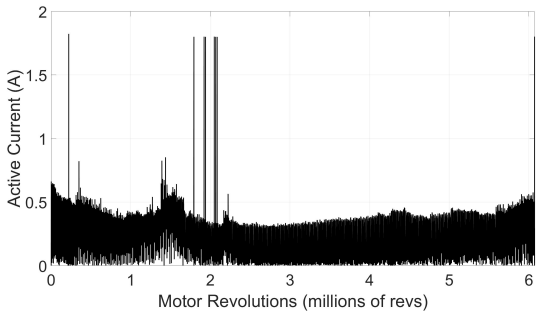

Figure 27. Mobility Actuator: TC4 Active Current

The various spikes in the current of the mobility actuator (Figure 27) during TC4 ConOps testing were believed to be a similar failure as what was observed during the TC3 accelerated life test. However, the mobility actuator was not physically dissassembled between restarts of the TC4 test. The test was able to be manually restarted and continued between current peaks.

Excavation Actuator—The excavation actuator successfully completed 1,083,342 motor revolutions during a single TC4 ConOps test using the transient thermal profile provided by JPL.

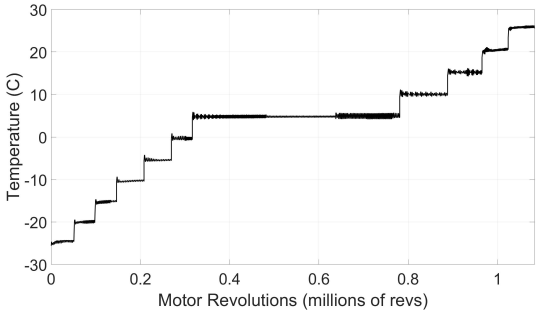

Figure 28. Excavation Actuator: TC4 Actuator Temperature

The temperature control can be seen in Figure 28.

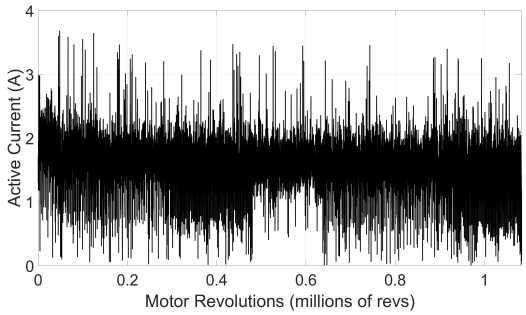

Figure 29. Excavation Actuator: TC4 Active Current

The active current of the excavation actuator during TC4 ConOps testing is shown in Figure 29. The noise and various current spikes in the data are believed to be the result of the ESI motor controller used to conduct tests. The motor controllers that will be used on mission have not been identified yet.

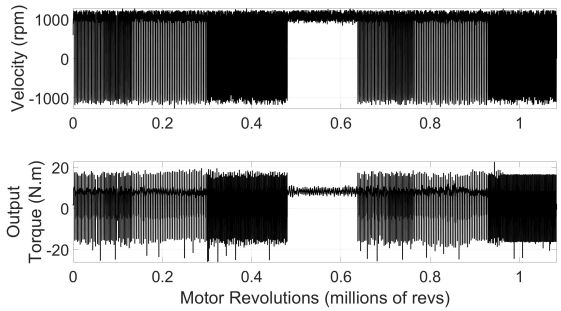

Figure 30. Excavation Actuator: TC4 Overview of Scheduler Performance

Figure 30 shows the velocity and output torque over the course of the TC4 ConOps test of the excavation actuator. There was a mistake within the scheduler that caused the actuator to hold 8.2 N.m at 1066 rpm over the course of approximate 1 million motor revolutions.

Shoulder Actuator—The shoulder actuator ConOps has not been completed yet.

9. Lessons Learned and Actuator Redesign

During assembly and testing of the TRL5 mobility, shoulder, and excavation actuators a few issues were identified. Modifications of the actuators were designed to address the issues. The accelerated life and ConOps tests will be repeated with the new designs to demonstrate that issues were resolved.

The IPEx actuators originally had 3 stages of dust sealing: labyrinth seal, Nomex felt seal, and a Teflon seal. The SKF carbon impregnated Teflon seals were hard to install properly and tended to fold over during installation. This installation issue is mostly attributed to improper installation direction. After installation there is no way to perform a visual inspection of the Teflon seal. After testing the Teflon seal showed significant wear and degradation. This was either due to improper installation or potentially the carbon impregnation not performing as expected. During the ConOps, where regolith was applied to the output of the actuators, the felt seals exceeded our expectations for the arm and excavation actuator.

The mobility actuator showed appreciable wear in the felt seal, but very little regolith propagated inside the actuator. The mobility actuator felt seal only showed more wear due to the total revolutions compared to the arm and excavation actuator. Due to the success of the felt seals it was decided to remove the Teflon seal. To address the wear of the felt seal in the mobility actuator an additional felt seal will be added in the redesign.

The felt seals were compressed 20% and successfully stopped regolith intrusion. However, the felt showed signs of flaring which implies the compression is too high. In future redesigns a compression of 10

During accelerated life testing of the mobility actuator the motor reached a current limit. Initially the actuator was removed from the test chamber and inspected, but there was no obvious explanation of why the current limit was reached, so the test was restarted. After continuing the accelerated life test, it was observed that the deep groove ball bearings used to support the motor rotor axially shifted towards the harmonic components by compressing the springs used to apply a light preload to the bearings. The springs were sized to exceed the axial force that the harmonic wave generator creates during operation, where Harmonic supplies an estimating equation . The torque used to estimate the axial force was conservatively selected to be the max momentary torque of the harmonic with a 1.5 FS applied. This axial movement allowed the wave generator to move deeper into the flex cup.

The accelerated life test was completed and ultimately reached 6,547,036 motor revolutions, but only after several restarts and some modifications. The initially the reason from the propagation of the wave generator was as determined to be due to the wave generator only being greased plated , which allowed the interface between the wave generator band and the inner of the flex cup to create friction leading the galling. This galling potentially acted like a screw forcing the wave generator to compress the rotor springs. It was decided that more grease be added between the interface wave generator and flex cup near the wave generator. This addition of grease is very similar to the grease recommendation in the harmonic drive manual. It was later determined that the deep groove ball bearings that were selected also had too much radial play. The bearing separation distance was also very small. The radial play issues and separation distance led to the rotor shaft displaying an appreciable wobble. Considering the galling and rotor wobble the motor rotor bearings were redesigned.

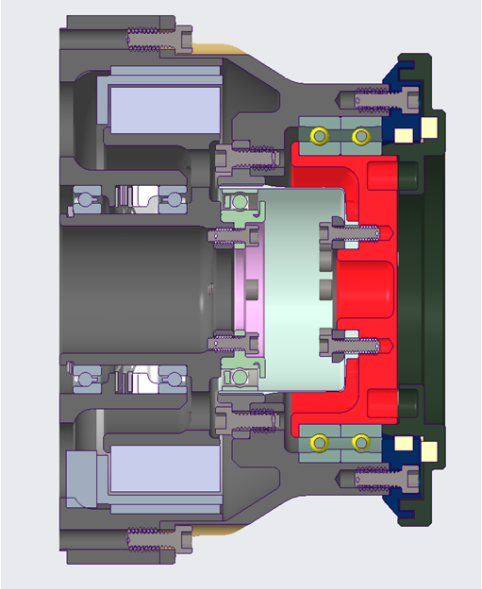

Figure 31. Mobility Actuator - Cross-section of the Redesign

The cross section in Figure 31 shows the new angular contact bearings for the motor rotor.

The new bearings also achieve a larger separation distance by moving the preload springs between the bearings. When the wave generator creates axial force, it can generate force into and out of the flex. The harmonic drive manual describes the force direction during acceleration and constant velocity as a force into the flex cup and during deceleration an axial force out of the flex cup. During, the Con-Ops of the IPEx mission there is equal amounts of acceleration and deceleration but extended periods of driving at constant velocity. Due to the unbiased load direction a new rotor bearing configuration redirects the load path into the rear bearing. On the previous design the springs reacted the load in this direction. Due to the self-aligning nature of the angular contact bearings and larger separation distance the rotor shaft wobble is believed to be addressed. The arm and excavation actuators will also be redesigned with a similar angular contact bearing and spring configuration after testing of the mobility actuator proves the changes to be effective.

The mobility actuator electrical power and heat generation needed optimization. It was determined that during the 30 cm/s driving speed the mobility actuator required 25 Watts of power and generated 20 Watts of heat. This is mostly due to the motor speed of 1530 rpm required to achieve 30 cm/s with a harmonic gear ratio of 80:1. If the gear ratio is reduced to 50:1 and the motor upsized to the LSI 75-20, the mobility actuator can reduce the required power to 12 Watts of electrical power and 9 Watts of heat generation. Since the Con-Ops required approximately 70 km of driving at the speed of 30 cm/s this gear ratio and motor stack length change was included in the redesign of the mobility actuator. The mobility actuator also showed some signs of wear in the harmonic gear teeth. This wear may have been amplified due to rotor issues detailed above, but it was determined that filling the root of the harmonic gear teeth instead of only grease plating may help with wear. This additional grease did not show any appreciable signs of increase drag.

10. SUMMARY

The development and testing of the mobility, shoulder, and excavation actuators provided valuable insights into their performance, identified challenges, and informed necessary design improvements.

The characterization tests aimed to empirically derive equations predicting the output torque of each actuator under varying conditions. The dependent variable, output torque, was influenced by independent factors such as motor speed, active current, bus voltage, and motor temperature. It was observed that temperature had a notable impact on active current across different torque and velocity profiles. The analysis revealed that voltage variation had minimal effect on active current, prompting a shift to using a single voltage for future tests. The empirical equations developed will play a crucial role in real-time torque predictions during the mission.

The accelerated life tests assessed the durability and reliability of the actuators under conditions simulating extreme operational loads. Each actuator demonstrated the capability to exceed mission requirements for input revolutions, achieving notable performance metrics. The mobility actuator successfully operated over 6.5 million motor revolutions, though the test had to be restarted several times due to axial movement of the rotor. This finding highlighted the need for design adjustments to mitigate issues related to bearing performance and friction.

The ConOps tests simulated mission scenarios based on expected thermal profiles and dust loading conditions. The mobility actuator completed extensive testing with multiple restarts, successfully accumulating over 6 million motor revolutions. The excavation actuator also performed admirably, completing over 1 million revolutions. These tests validated the actuators' resilience and operational readiness, though they revealed some challenges, particularly concerning current spikes and thermal management that need to be addressed before the mission.

Several design enhancements emerged from the testing results. The original sealing system of the actuators proved to be problematic, especially the Teflon seal, as it showed significant wear. The Teflon seals were therefore removed, while the felt seals were kept, as they prevented regolith intrusion well. Future designs will reduce the compression of felt seals to prevent wear while maintaining dust protection.

Furthermore, the bearings supporting the motor rotor exhibited issues with axial movement, prompting a redesign to include angular contact bearings that can better handle load distribution. This new configuration aims to reduce wobble and improve overall stability during operation. In addition, power optimization strategies were recommended, including adjustments to the gear ratio and motor specifications. Switching to a 50:1 gear ratio and upsizing the motor are expected to lower power requirements and heat generation during operation, aligning with the mission's long-distance driving needs.

The iterative nature of the testing and design process was crucial for identifying and resolving issues as they arose. The project emphasized the need for rigorous testing under various environmental conditions to ensure actuator reliability. Real-time monitoring and prompt decision-making during tests were vital for adapting to unexpected challenges, highlighting the importance of flexibility in engineering design.

APPENDICES

Table 1. TC1 & TC2 Test Plan for the Mobility Actuator

Step	Load (N.m)	Speed (rpm)	Duration
Acceleration: 100 rpm/s			
0	0	±1700:200:100 ±50, ±25, ±10	30s (per speed)
1	15	±1700:200:100 ±50, ±25, ±10	30s (per speed)
2	12	±1700:200:100 ±50, ±25, ±10	30s (per speed)
3	9	±1700:200:100 ±50, ±25, ±10	30s (per speed)
4	6	±1700:200:100 ±50, ±25, ±10	30s (per speed)
5	3	±1700:200:100 ±50, ±25, ±10	30s (per speed)
6	0	±1700:200:100 ±50, ±25, ±10	30s (per speed)

Table 2. TC1 & TC2 Motor Characterization Test Plan for the Excavation and Shoulder Actuator

Step	Load (N.m)	Speed (rpm)	Duration
Acceleration: 100 rpm/s			
0	0	±200:200:2000	10s (per speed)
1	5:5:50	±200	10s (per torque)
2	5:5:50	±400	10s (per torque)
3	5:5:50	±600	10s (per torque)
4	5:5:50	±800	10s (per torque)
5	5:5:50	±1000	10s (per torque)
7	5:5:50	±1200	10s (per torque)
8	5:5:50	±1400	10s (per torque)
9	5:5:50	±1600	10s (per torque)
10	5:5:50	±1800	10s (per torque)
11	5:5:50	±2000	10s (per torque)
12	0	±200:200:2000	10s (per torque)

Table 3. TC3 Accelerated Life Test Plan for the Mobility Actuator

Step	Load (N.m)	Speed (rpm)	Duration
Acceleration: 500 rpm/s			
0	0	1000	1,000 motor revs
1	2.69	+1530	50,0000 motor revs
2	2.69	-1530	50,0000 motor revs
3	Continue Steps 1 & 2 until failure or 11,400,000 motor revs are reached		
4	If 11,400,000 motor revs are reached run Step 0 then stop test		

Table 4. TC3 Accelerated Life Test Test Plan for the Excavation Actuator

Step	Load (N.m)	Speed (rpm)	Duration
Acceleration: 100 rpm/s			
0	0	200:200:2000	10s (per speed)
1	40	+1066	250,0000 motor revs
2	40	-1066	250,0000 motor revs
3	Continue Steps 1 & 2 until failure or 2,000,000 motor revs are reached		
4	If 2,000,000 motor revs are reached run Step 0 then stop test		

Table 5. TC3 Accelerated Life Test Plan for the Shoulder Actuator

Step	Load (N.m)	Speed (rpm)	Duration
Acceleration: 100 rpm/s			
0	0	500	10s
1	18.5	+500	100,0000 motor revs
2	18.5	-500	100,000 motor revs
3	Continue Steps 1 & 2 until failure or 2,000,000 motor revs are reached		
4	If 2,000,000 motor revs are reached run Step 0 then stop test		

Table 6. TC4 ConOps Test Plan for the Mobility Actuator

Step	Load (N.m)	Speed (rpm)	Duration (Motor Revs)	Cases
Acceleration: 100 rpm/s Perform No Load at Ambient Temperature				
0	0	+1000	+1000	Pre-Test No Load
Test starts at -35C Initial temperature set point ±5C Free error margin for other temperatures				
1	1.5	+1530	+8500	Torque to drive to excavation site
2	1.1	+64	+135	Torque to drive while excavating
3	2.7	-1530	-8500	Torque to drive to dump site after excavation
4	**Repeat Steps 1 through 3 (7 times)**			
5	**Increase temperature by 5C**			
6	**Go back to Step 4 (until 45C is reached)**			
7	**Hold 45C Repeat Steps 1 through 3 (112 times)**			
8	**Decrease temperature by 5C**			
9	**Repeat Steps 1 through 3 (9 times)**			
10	**Decrease temperature by 5C**			
11	**Go back to Step 9 (until -15C is reached)**			
12	0	+1000	+1000	Post-Test No Load

Table 7. TC4 ConOps Test Plan for the Excavation Actuator

Step	Load (N.m)	Speed (rpm)	Duration (Motor Revs)	Cases
Acceleration: 100 rpm/s Test starts at -25C Initial temperature set point ±5C Free error margin for other temperatures				
0	0	+1000	+1000	Pre-Test No Load
1	8.2	+1066	+2256	Average torque to excavate
2	16.38	+1066	+36	Torque Peak during excavation
3	1	-1040	-388	Torque to dump
4	**Repeat Steps 1 through 3 (16 times)**			
5	**Increase temperature by 5C**			
6	**Go back to Step 4 (until 5C is reached)**			
7	**Hold 5C Repeat Steps 1 through 3 (111 times)**			
8	**Increase temperature by 5C**			
9	**Repeat Steps 1 through 3 (28 times)**			
10	**Increase temperature by 5C**			
11	**Go back to Step 9 (until 25C is reached)**			
12	0	+1000	+1000	Post-Test No Load

Table 8. TC4 ConOps Test Plan for the Shoulder Actuator

Step	Load (N.m)	Speed (rpm)	Duration (Motor Revs)	Cases
Test starts at -10C Initial temperature set point ±5C Free error margin for other temperatures				
0	0	+500	+500	Pre-Test No Load
1	25	+200	+40	Offloading from lander
2	3.8	-260	-20	Unloaded 45°to 0°
3	18.5	+500	+4.5	Excavating
4	18.5	-500	-4.5	Excavating
Repeat Steps 3 through 4 (112 times)				
5	13	+260	+20	Loaded 0°to 45°
6	**Repeat Steps 2 through 5 (18 times)**			
7	**Increase temperature by 5C**			
8	**Go back to Step 6 (until 20C is reached)**			
9	**Hold 20C Repeat Steps 2 through 5 (115 times)**			
10	**Decrease temperature by 5C**			
11	**Repeat Steps 2 through 5 (22 times)**			
12	**Go back to Step 10 (until -5C is reached)**			
13	0	+500	+500	Post-Test No Load

ACKNOWLEDGMENTS

The entire Swamp Works family and their individual contributions to the IPEx project

REFERENCES

[1] R. P. Mueller, J. D. Smith, J. M. Schuler, A. J. Nick, N. J Gelino, K. W. Leucht, I. I. Townsend, and A. G. Dokos, "Design of an Excavation Robot: Regolith Advanced Surface Systems Operations Robot (RASSOR) 2.0x", *2016 ASCE Earths & Space Conference*, 2016.

[2] J. M. Schuler, A. J. Nick, J. D. Smith, K. W. Leucht, and A. G. Langton, "ISRU Pilot Excavator: Bucket Drum Scaling Experimental Results", *ASCE Earth and Space Conference 2022*, 2022.

[3] R. P. Mueller, A. J. Nick, J. M. Schuler, and J. D. Smith, "Zero horizontal reaction force excavator", 9027265, May 12, 2015.

[4] B. C. Buckles, J. M. Schuler, A. J. Nick, J. D. Smith and T. J. Muller, "ISRU Pilot Excavator - Development of Autonomous Excavation Algorithms", *NASA Technical Reports*, 2022.

[5] J. M. Schuler, et al, "ISRU Pilot Excavator (IPEx)

Technology Readiness Level 5 Design Overview", *AIAA AVIATION FORUM AND ASCEND 2024*, 2024.

[6] R. P. Mueller, et al, "NASA KSC Swamp Works: Methodology and Technology Development Summary", *ASCE Earth and Space Conference 2021*, 2021.

[7] C. J. Clark, J. D. Smith, A. J. Nick, V. Ortega, A. Kennett, R. P. Dillon, and B. Buckles, "Experimental Capabilities and Achievements of the Space Environment Dynamometer (SED)", *2023 IEEE Aerospace Conference*, 2023.

[8] NASA Online Directives Information System (NODIS) website: https://soma.larc.nasa.gov/simplex/pdf_files/N_PR_8705_0004.pdf.

[9] NASA website: https://www.nasa.gov/wp-content/uploads/2017/03/std8070.1.pdf.

BIOGRAPHY

Casey Clark *received a B.S. and M.S. in Aerospace Engineering from Florida Institute of Technology in 2016 and 2018, respectively. He is the lead test engineer at Swamp Works NASA Kennedy Space Center. His interests include nonlinear control systems, multivariable feedback control systems, cryobotics and robotic design.*

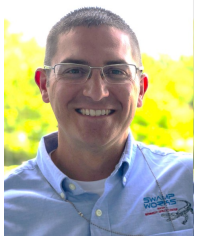

Drew Smith *is a robotics engineer, Principal Investigator, and a founder of Swamp Works at Kennedy Space Center. He began working for NASA in 2009 after receiving a B.S. in Mechanical Engineering from the University of North Florida. He is a subject matter expert in off earth excavation and has designed and tested multiple percussive excavation end effectors for NASA's Jet Propulsion Laboratory, Glenn Research Center, and Johnson Space Center. He is also an inventor of patented extraterrestrial mining robots for in situ resource utilization. Drew is currently the Lead Design Engineer for Swamp Works.*

Andrew Nick *received a B.S. in Mechanical Engineering from Florida Institute of Technology in 2007. He was a contractor for NASA at the Kennedy Space Center for over 13 years before converting to civil servant in 2020. As a founding member of Swamp Works at KSC, he has spent most of his career developing robotic systems for exploration and resource utilization of planetary surfaces. He is an SME in the Granular Mechanics and Regolith Operations (GMRO) laboratory.*

Victoria Ortega *received a B.S. in Mechanical Engineering from Carnegie Mellon University in 2022. She worked in Swamp Works at NASA Kennedy Space as a co-op in 2021 and started her full-time career in 2022. Since then, she has assumed roles as a lead design and test engineer while supporting ISRU Pilot Excavator and other projects.*

Jason Schuler *is a mechanical engineer and founding member of Swamp Works – a team at Kennedy Space Center devoted to developing robotic technologies to use space resources. He is a co-inventor of RASSOR - aka Regolith Advanced Surface Systems Operation Robot and has spent the last 16 years developing technologies that will interact with extra-terrestrial regolith. Jason is currently the Principal Investigator for the ISRU Pilot Excavator project to develop a robotic system to demonstrate large scale lunar regolith excavation on the moon.*

Jeffrey Dyas *is a systems engineer at NASA's Kennedy Space Center, where he has worked since 2016. He received a B.Sc. in mechanical engineering from Auburn University in 2014, M.Sc. in Industrial and Systems Engineering from University of Alabama in Huntsville in 2016, M.Sc. in Industrial and Organizational Psychology from University of Alabama in Huntsville in 2018, and M.Sc. in Aerospace Systems Engineering from University of Alabama in Huntsville in 2019. His research focuses on alternative methods requirement-based system design using value-based design via system level optimization of stakeholder preferences. He currently supports multiple projects at KSC as a systems engineer, including ISRU Pilot Excavator, CLPS Electrodynamic Dust Shield, and Moon 2 Mars Pre-Formulation Model-based Systems Engineering Team.*

John Lahl *served his country for 30 years in the US Air Force as a Jet Engine Specialist, retiring in 2013. He is the Lab Senior Engineering Technician at Swamp Works NASA Kennedy Space Center. His interests include Aviation and Space related machinery and design.*